

Resonant spatiotemporal learning in large random recurrent networks

Emmanuel Dauce¹, Mathias Quoy², Bernard Doyon³

¹ Movement and Perception (UMR6559), Faculty of Sport Science, University of the Mediterranean, 163, avenue de Luminy, CP 910, 13288 Marseille cedex 9, France

² Neurocybernetics team, ETIS, UCP-ENSEA, 6, avenue du Ponceau, 95014 Cergy-Pontoise cedex, France

³ Unité INSERM U455, Service de Neurologie-CHU Purpan, 31059 Toulouse cedex, France

Received: 27 April 2001 / Accepted in revised form: 15 January 2002

Abstract. Taking a global analogy with the structure of perceptual biological systems, we present a system composed of two layers of real-valued sigmoidal neurons. The primary layer receives stimulating spatiotemporal signals, and the secondary layer is a fully connected random recurrent network. This secondary layer spontaneously displays complex chaotic dynamics. All connections have a constant time delay. We use for our experiments a Hebbian (covariance) learning rule. This rule slowly modifies the weights under the influence of a periodic stimulus. The effect of learning is twofold: (i) it simplifies the secondary-layer dynamics, which eventually stabilizes to a periodic orbit; and (ii) it connects the secondary layer to the primary layer, and realizes a feedback from the secondary to the primary layer. This feedback signal is added to the incoming signal, and matches it (i.e., the secondary layer performs a one-step prediction of the forthcoming stimulus). After learning, a resonant behavior can be observed: the system resonates with familiar stimuli, which activates a feedback signal. In particular, this resonance allows the recognition and retrieval of partial signals, and dynamic maintenance of the memory of past stimuli. This resonance is highly sensitive to the temporal relationships and to the periodicity of the presented stimuli. When we present stimuli which do not match in time or space, the feedback remains silent. The number of different stimuli for which resonant behavior can be learned is analyzed. As with Hopfield networks, the capacity is proportional to the size of the second, recurrent layer. Moreover, the high capacity displayed allows the implementation of our model on real-time systems interacting with their environment. Such an implementation is reported in the case of a simple behavior-based recognition task on a mobile robot. Finally, we present some functional analogies with biological systems in terms of autonomy and dynamic binding, and present some hypotheses on the computational role of feedback connections.

Correspondence to: E. Dauce
(e-mail: dauce@esm2.imt-mrs.fr)

1 Introduction

Understanding global dynamics of the brain in functional terms is a central issue in neurophysiology. Depending on the spatial scale, one can consider neuronal, local-field, or global-field dynamics, and study the temporal behavior of neurons or groups of neurons. Measures of complexity (Skarda and Freeman 1987), temporal coincidence (Abeles et al. 1993), local synchronization (Gray and Singer 1989), and long-range synchronization (Rodriguez et al. 1999) lead to the idea that perception and/or cognition rely on collective organization phenomena. Such organization (i) manifests in reproducible spatio-temporal patterns of firing that take place on a millisecond timescale (Abeles et al. 1993; MacLeod and Laurent 1996), (ii) is distributed throughout a whole sensory structure (Skarda and Freeman 1987; MacLeod and Laurent 1996) or the whole brain (Rodriguez et al. 1999), and (iii) is transient, i.e., desynchronization follows synchronization (Schillen and König 1991; Rodriguez et al. 1999).

This collective organization depends partly on the input sensory signal, but also (which is the point we want to stress) on inner dynamical constraints. For instance, the change in the dynamics following input presentation is not coded in the input signal; it arises as a phase transition (Skarda and Freeman 1987) in the dynamics of the inner system. This transition depends on (i) a long past history and adaptation between this particular stimulus and the system, and (ii) an inner dynamical context that may modulate the way in which a given stimulus is interpreted.

An artificial neural network with inner recurrent links can be seen as a dynamic system as it can generate an inner signal that propagates through inner (or recurrent) interactions. We call such a system a dynamic neural network. In order to perform computation with recurrent networks, people often try to avoid interferences between inner signal and input (command) signal. For instance, in

classical applications of recurrent networks (Williams and Zipser 1989; Elman 1990), inner recurrent states work as buffers that memorize a context, but one tries to avoid active inner dynamics for the response to be specified by the input signal (i.e., the same input sequence always produces the same response). On the other side, the classical Hopfield (1982) model and derivatives (Herz et al. 1989) are autonomous dynamic systems (i.e., there is no interaction in real time with an input signal), and the final attractor thus strictly depends on the initial conditions.

In this article, we present an alternative approach in the framework of a dynamic neural network’s computation. We have made the choice to use a model which is simple in its design, and highly complex in its behavior. Our idea is that such a generic system could shed some new light on natural processes of perception. So, more than the implementation details of our model, what are important are its following characteristics:

1. *Dynamics* varying from fixed point to chaos depending on the system parameters and/or input and learning.
2. *Structure* composed of two layers enabling a resonance phenomenon.
3. *Learning* scheme storing spatiotemporal dependencies.
4. *Computational* efficiency as well as partly *theoretical* tractability.
5. *Real-world* implementation in a robotic control architecture.

We present in Sect. 2 the generic structure of a multipopulation random recurrent model, with an on-line rule for weight adaptation. Then, taking a global analogy with biological sensory systems, we present in Sect. 3 a model with a “primary” layer and a “secondary” layer, called *ReST* (for resonant spatiotemporal system). In Sect. 4, we show the effects of the learning rule, as a reduction of the dynamics on the secondary layer, and a feedback strengthening from the secondary layer towards the primary layer. We then study the retrieval ability and the capacity of the model. Then we present in Sect. 5 an example of artificial system design in the case of robot navigation and scene recognition. This preliminary experiment illustrates the ability of our system to deal with real-world data. Finally, we draw in Sect. 6 parallels between the functioning of our model and biological observations, in terms of chaos, dynamic binding, and cortical and subcortical structures, and discuss temporal scales.

2 Multipopulation recurrent model

The class of neural networks we start from are recurrent systems, whose weights are set according to a random draw (random recurrent neural networks). We present in this section a generic formalism for the design of multipopulation random recurrent systems. This formalism will help to specify the sensory architecture we use in Sect. 3.

Random neural networks were introduced by Amari (1972) in a study of their large size properties. Predictions

of the mean field of such systems can be obtained in the limit of large sizes under an hypothesis of independence of the individual signals (Sompolinsky et al. 1988; Cessac 1995). This convergence towards mean-field equations has recently been formally proved (Moynot and Samuelides 2002). The arising of several sorts of synchronized dynamics can thus be proven in a model with excitatory and inhibitory populations (Daucé et al. 2001).

Here we will mainly consider our random networks as finite-size dynamic systems, that can display a generic quasiperiodicity route to chaos with a continuous tuning of gain parameter (Doyon et al. 1993). Note that dynamic neural networks have some specific time constraints that distinguish them from pure feedforward associative systems. In particular, the time necessary to reach an attractor is not determined – one needs “several time steps” or “a certain time” to reach the neighborhood of the attractor. This transient time, which may be short, is necessary, and takes place as soon as a change occurs in the environment of the system.

2.1 Activation dynamics

Our dynamic system (1) is defined as a pool of P interacting populations of neurons, of respective sizes $N^{(1)}, \dots, N^{(P)}$. The global number of neurons is $N = \sum_{p=1}^P N^{(p)}$. The synaptic weights from population q towards population p are stored in a matrix $\mathbf{J}^{(pq)}$ of size $N^{(p)} \times N^{(q)}$. The state vector of population p at time t is $\mathbf{x}^{(p)}(t)$, of size $N^{(p)}$. The initial conditions $\mathbf{x}_i^{(p)}(0)$ are set according to a random draw uniform in $[0, 1]$.

At each time step $t \geq 1$, $\forall (p, q) \in \{1, \dots, P\}^2$, $\forall i \in 1, \dots, N^{(p)}$,

$$h_i^{(pq)}(t) = \sum_{j=1}^{N^{(q)}} J_{ij}^{(pq)} x_j^{(q)}(t-1)$$

is the local field of population q towards neuron i . This variable measures the influence of a particular population on the activity of a given neuron.

We also consider spatiotemporal input signals $\mathbf{I}^{(p)} = \{\mathbf{I}^{(p)}(t)\}_{t=1, \dots, +\infty}$, where $\mathbf{I}^{(p)}(t)$ is a $N^{(p)}$ -dimensional input vector at time t on population p . The input $\mathbf{I}^{(p)}(t)$ acts like a bias on each neuron (in contrast to the Hopfield system, the input does not correspond to the initial state $\mathbf{x}_i^{(p)}(0)$ of the network). Then, the global equation of the dynamics is

$$\forall t \geq 1, \quad \forall p \in \{1, \dots, P\}, \quad \forall i \in \{1, \dots, N^{(p)}\}$$

$$\begin{cases} u_i^{(p)}(t) = -\theta^{(p)} + \sum_{q=1}^P h_i^{(pq)}(t) \\ x_i^{(p)}(t) = f_g[u_i^{(p)}(t) + I_i^{(p)}(t)] \end{cases} \quad (1)$$

The activation potentials $u_i^{(p)}$ have real continuous values, and correspond to a linear combination of afferent local fields minus activation threshold $\theta^{(p)}$. The activation states $x_i^{(p)}(t)$ are continuous and take their values in $[0, 1]$, with a nonlinear transfer function

$f_g(u) = (1 + \tanh(gu))/2$, whose gain is $g/2$. We call the “pattern of activation” the spatiotemporal signal $\mathbf{x}^{(p)}$ corresponding to the exhaustive description of a trajectory of the system’s dynamics in layer p .

An important characteristics of our system is the random nature of the connectivity pattern. We suppose that the distribution of the connection weights follow the Gaussian law $\mathcal{N}[0, (\sigma_J^{(pq)})^2/N^{(q)}]$, so that $E[\text{var}(\sum_{j=1}^{N^{(q)}} J_{ij}^{(pq)})] = (\sigma_J^{(pq)})^2$. This random draw implies that our synaptic weights are almost surely nonsymmetric. This nonsymmetry is a necessary requirement for having complex dynamics.

As the local fields $h_i^{(pq)}$ are updated synchronously, the global dynamics (Eq. 1) also obeys to a synchronous update. Then the state of the system at time t both depends on the state of the system at time $t-1$ and the input $\mathbf{I}(t)$ (at time t). One can thus notice that (i) the transmission delay is uniformly equal to 1, and (ii) our system is deterministic as soon as the input signal is set according to a deterministic process.

2.2 Learning dynamics

We extend here the activation dynamics to a generic on-line learning dynamics. A first article (Daucé et al. 1998) presented a Hebbian learning process in a nonstructured random recurrent neural network that was found to reduce the complexity of the dynamics (called “dynamics reduction” in Sect. 4.3). We propose here a local Hebbian learning rule that relies on an on-line estimate of the covariance between afferent and efferent signals, as in Sejnowski (1977). We will suppose hereafter that we have at each time step local estimates of the mean activation, which are stored in vector $\hat{\mathbf{x}}(t)$ and updated according to $\hat{\mathbf{x}}(t) = (1 - \beta)\hat{\mathbf{x}}(t-1) + \beta\mathbf{x}(t)$, and we take $\beta = 0.1$ in our simulations.

The learning dynamics is thus described by the following set of equations:

$$\begin{aligned} \forall t \geq 1, \quad \forall (p, q) \in \{1, \dots, P\}^2, \\ \forall i \in \{1, \dots, N^{(p)}\}, \quad \forall j \in \{1, \dots, N^{(q)}\} \end{aligned}$$

$$\begin{cases} u_i^{(p)}(t) = -\theta^{(p)} + \sum_{r=1}^P \sum_{k=1}^{N^{(r)}} J_{ik}^{(pr)}(t-1)x_k^{(r)}(t-1) \\ x_i^{(p)}(t) = f_g[u_i^{(p)}(t) + I_i^{(p)}(t)] \\ J_{ij}^{(pq)}(t) = J_{ij}^{(pq)}(t-1) \\ \quad + \frac{\varepsilon^{(pq)} \phi_g(u_i^{(p)}(t))}{N^{(q)}} [x_i^{(p)}(t) - \hat{x}_i^{(p)}(t)] \\ \quad \times [x_j^{(q)}(t-1) - \hat{x}_j^{(q)}(t-1)] \end{cases} \quad (2)$$

where $\phi_g(u) = [1 - f_g(u)]$ is a function that prevents weight drift when the postsynaptic neuron is saturated, and $\varepsilon^{(pq)}$ is the learning parameter from population q

towards population p (assumed to be small). Note that we take into account the discrete time delay between presynaptic neuron j and postsynaptic neuron i , which is important for learning temporal dependencies (Herz et al. 1989).

3 ReST model

3.1 A two-layer perceptual model

We have designed our ReST model to enable study of the interplay between a fully recurrent system and a spatiotemporal signal. The design of this architecture has been guided by two objectives: (i) to give some insights in the global functioning of biological perceptual systems, and (ii) to lead to real-world applications (see Sect. 5).

The analogy with biological sensory structures is the following: we consider that a recognition process (e.g., odor on visual scene) may rely on the interplay between several structures, which are partly autonomous and that correspond to different levels of generalization. Primary layers may produce basic treatments, while deeper (secondary) layers may correspond to a global treatment, linking spatial and temporal context of perception, and taking into account the memory of learned stimuli. The recognition of a given stimulus may then depend on the coherence (or dynamic coupling) between primary layers and secondary (and deeper) layers. Note that our point of view is distinct (and possibly complementary) from the feedforward approach, see for instance Thorpe et al. (1996).

We define an architecture with two layers (i.e., $P = 2$): a primary layer of index 1 and a secondary layer of index 2. Population sizes $N^{(1)}$ and $N^{(2)}$ are supposed large (100–2000 neurons in our simulations) and are not necessarily equal. This system is simple in its design, but may produce complex dynamic behaviors. The two-layer architecture is shown in Fig. 1. We can define three important classes of links: “feedforward links” $\mathbf{J}^{(21)}$ propagate the input signal towards the secondary layer, “inner links” $\mathbf{J}^{(22)}$ generate inner signals, and “feedback links” $\mathbf{J}^{(12)}$ send back the activity of the secondary layer towards the primary layer. In this model, primary lateral links $\mathbf{J}^{(11)}$ are equal to zero.

3.2 Spontaneous dynamics

We call “spontaneous dynamics” the dynamics corresponding to Eq. (1), when the weights have been defined according to a random draw (there is no learning). As we use rather large systems, the behavior of a given system is supposed to be representative of the behavior of a whole family of random systems that have been defined according to the same parameters set. This assumption is only exact at the limit of large sizes (Moynot and Samuelides 2002). We have checked the reproducibility and genericity of the behaviors described hereafter on several networks of finite size.

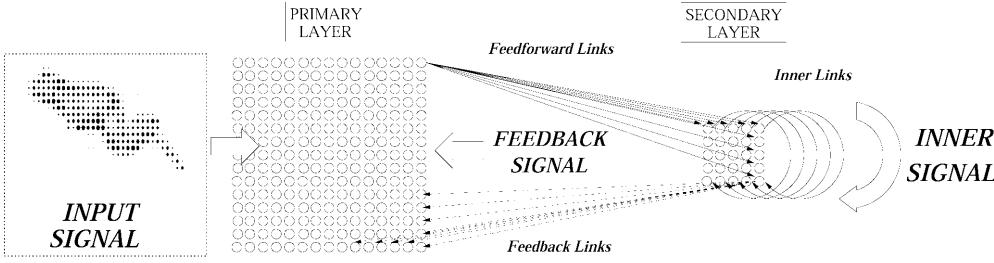


Fig. 1. Architecture of the ReST (resonant spatiotemporal system) model. Our model is composed of two layers, whose sizes are not necessarily equal. Only a few of the links are represented (links are monodirectional). The *primary layer* is subjected to a spatiotemporal

input pattern $\mathbf{I}^{(1)}$; the *secondary layer* has no input signal. The activity of the secondary layer (inner signal) is chaotic. The activity in the primary layer depends both on the input signal and the *feedback signal* from the secondary layer

The mean field equations (Cessac 1995) have helped us to determine the parameters of the system (the parameters are displayed in Table 1). The parameters have been chosen for the inner dynamics to be chaotic, so that the response of the system is not fully specified by the input sequence. More precisely, taking into account the sparsity of the input signal, the value of $\sigma_j^{(21)}$ is chosen such that the feedforward local-field mean standard deviation $E[\sigma(\{h_i^{(21)}(t)\}_{i=1,\dots,+\infty})]$ equals 0.2. With setting $\sigma_j^{(22)} = 1$, the mean field equations allow prediction that $E[\sigma(\{h_i^{(22)}(t)\}_{i=1,\dots,+\infty})] \simeq 0.3$ at the thermodynamic limit, so that inner signal amplitude is significantly stronger than the feedforward signal amplitude. At a given time t , the spatial pattern of activation $x^{(2)}(t)$ is such that 15% to 20% of the neurons are active, i.e., have their activation $> 0.5(E[x_i^{(2)}(t)] \simeq 0.18$ at the thermodynamic limit). One can also note that almost every neuron is dynamically active in the secondary layer, i.e., 80% of the neurons have an activation signal $\{x_i^{(2)}(t)\}_{i=1,\dots,+\infty}$ whose standard deviation is > 0.1 .

3.3 Predictability

Only the primary layer is stimulated by a spatiotemporal input signal. The input signal is supposed sparse, and parameter $m_1^{(1)}$ denotes the input sparsity (the average proportion of neurons which are stimulated at each time). As the number of primary neurons is equal to the number of input channels, the activation signals of primary neurons are strongly correlated with their input signals. If we suppose moreover that the input signal is binary, i.e., $\forall i, \forall t, I_i^{(1)}(t) \in \{0, 1\}$, the primary pattern of

activation $\mathbf{x}^{(1)}$ and the input signal $\mathbf{I}^{(1)}$ have almost the same values. On the contrary, there is no spatial matching between the primary pattern of activation $\mathbf{x}^{(1)}$ (and/or the input signal $\mathbf{I}^{(1)}$) and the secondary pattern of activation $\mathbf{x}^{(2)}$.

One can, however, remark that primary and secondary patterns of activation are not independent (due to the weights couplings between the two layers). In other words, the dynamics that takes place in secondary layer is partly predictable, knowing primary-layer activity. This statistical dependency can be observed if our system is submitted to a periodic input signal $\mathbf{I}^{(1)}$ of period τ so that $\forall t, \mathbf{I}^{(1)}(t + \tau) = \mathbf{I}^{(1)}(t)$ (see Fig. 2). In that case, the chaotic dynamics in the secondary layer has a residual periodicity, i.e., $\forall t, \text{cor}[\mathbf{x}^{(2)}(t), \mathbf{x}^{(2)}(t + \tau)] \simeq 0.6$. This mutual periodicity makes it possible to associate the periodic primary pattern of activation $\mathbf{x}^{(1)}$ to the periodically distributed secondary pattern of activation $\mathbf{x}^{(2)}$ (comparable to a cyclostationary random process). So, in the case of periodic input signals, primary and secondary layers display a *weak dynamic coupling*, i.e., one can predict the distribution of secondary layer activations from knowledge of the primary pattern of activation. This statistical predictability allows learning of spatiotemporal associations between the two layers, and will be used in Sect. 4.

Note, however, that secondary-layer chaotic dynamics is not equivalent to (and richer than) a random process. Indeed, we have remarked that the distribution of activations in the secondary layer is highly sensitive to small changes in the spatial and temporal characteristics of the input signal. One can observe a strong remapping in the secondary pattern of activation after a small

Table 1. Few parameters are necessary to define the initial system (ReST, resonant spatiotemporal system). The thresholds $\theta^{(1)}$ and $\theta^{(2)}$ are set strong enough to lower activity and avoid saturation. The feedforward links and inner links are randomly set according to $\mathcal{N}(0, (\sigma_j^{(21)})^2/N^{(1)})$ and $\mathcal{N}(0, (\sigma_j^{(22)})^2/N^{(2)})$ (the feedforward links are adapted to the statistics of the input signals, where $m_1^{(1)}$ corre-

sponds to the mean sparsity of the input signal). Initially (before training), feedback links are equal to zero, so that the secondary-layer activity has no influence on the primary layer. Lateral links in the primary layer are also equal to zero. Gain parameter $g = 8$ allows for chaotic dynamics in the secondary layer. Typical learning parameters are also given in the *right hand part* of the table (see text)

Parameters for the two-layer ReST model				Typical learning parameters		
Threshold	Weight standard deviations		Gain	Weight adaptation		Update rate of the mean activation
$\theta^{(1)} = 0.5$	$\sigma_j^{(11)} = 0$	$\sigma_j^{(12)} = 0$	$g = 8$	$\alpha^{(11)} = 0$	$\alpha^{(12)} = 0.1$	$\beta = 0.1$
$\theta^{(2)} = 0.4$	$\sigma_j^{(21)} = 0.2/\sqrt{m_1^{(1)}}$	$\sigma_j^{(22)} = 1$		$\alpha^{(21)} = 0$	$\alpha^{(22)} = 0.02$	

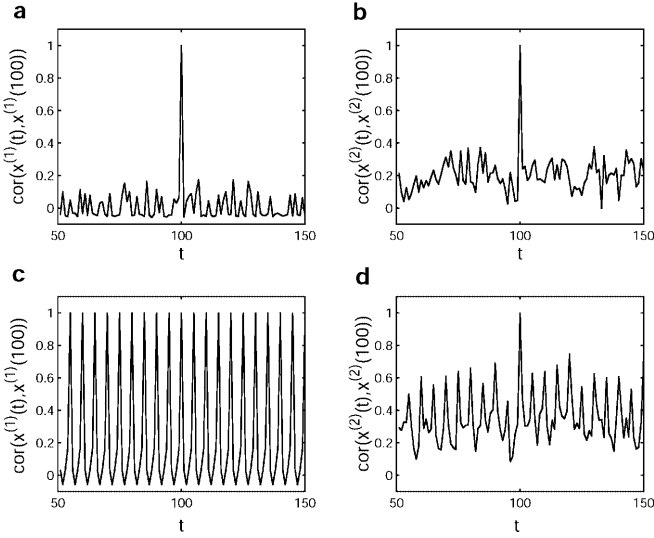


Fig. 2a-d. Measures of correlations between spatial patterns of activation, in primary and secondary layers, for (random) nonperiodic and periodic input signals. The activity of the system between $t = 51$ and $t = 150$ is shown. For $p \in \{1, 2\}$, $t \in 51, \dots, 150$, we measure the correlation between $\mathbf{x}^{(p)}(100)$ and $\mathbf{x}^{(p)}(t)$. $N^{(1)} = 200$ and $N^{(2)} = 200$; other parameters are in Table 1. **a** Nonperiodic (random) input signal, primary layer. **b** Nonperiodic (random) input signal, secondary layer. **c** Period-5 input signal, primary layer. **d** Period-5 input signal, secondary layer

change in the input signal. This denotes a *structural instability* of the dynamics (a spontaneous tendency to modify its inner dynamic organization). Before learning, our system is thus highly sensitive to noise or stimulus variations. It thus behaves in a very different manner than a system composed of stochastic units.

We have also remarked that signals with long periods (i.e., $\tau > 10-15$) lead to a secondary pattern of activation whose residual period is an harmonic of the input period. In that case, one can not have bijective associations between primary spatial patterns of activation and secondary spatial distributions of activation. In Sects. 4 and 5, we assume that input sequences have rather short periods, of 3–10.

4 Learning and retrieval

In classical “Hebbian” studies on single-population recurrent networks, connection weights are set according to a given set of predefined sequences (Herz et al. 1989; Gerstner et al. 1993) without dynamic interactions. On the contrary, our system uses an *on-line* learning rule, so that the weights are updated *at each time step* during the learning process. Weight adaptation is thus grounded on a real-time interaction between the input signal and the system dynamics. In order to evaluate the effect of the learning rule on the dynamics, we alternate learning phases (Eq. 2) and testing phases (Eq. 1).

A first attempt to learn sequential patterns of activation from a background chaotic activity with an on-line Hebbian learning can be found in Hertz and Prugel-Bennett (1996). Otherwise, a Hebbian learning

rule has been proposed in our model in Daucé et al. (1998) for the dynamic encoding of *static* input patterns.

For simulations of the ReST model, learning takes place on inner and feedback links, i.e., $\varepsilon^{(12)} = 0.1$ and $\varepsilon^{(22)} = 0.02$, so that the learning “strength” is lighter on secondary-layer recurrent links. Quantitative effects of parameter $\varepsilon^{(22)}$ on the learning capacity can be found in Sect. 4.3; otherwise, we have $\varepsilon^{(11)} = \varepsilon^{(21)} = 0$ (the weights from the primary layer remain unchanged).

4.1 Learning process

Let us now consider that the primary layer is continuously stimulated by a periodic signal $\mathbf{I}^{(1)}$ (repeated every τ time steps), and that the dynamics of the system is given by Eq. (2). Figure 3 presents the time evolution of the neural activity in population 2, while the system is submitted to a period-5 spatiotemporal input signal (for visual comfort, we have taken a pattern representing a frog jump).

During the learning process the synaptic weights are modified at each time step, so that the whole system continuously evolves under the constraint of the external signal $\mathbf{I}^{(1)}$. Two sorts of dynamic changes can thus be observed in the system (Fig. 3). First, the secondary-layer activity, which is initially chaotic, gets closer to a periodic behavior (Fig. 3a). The learning process tends to *reduce* the complexity of the initial chaotic dynamics towards a periodic dynamics (period-5 dynamics), so that the predictability between primary and secondary layers activities tends to increase. Nevertheless, changes in the weights remain very weak, and the statistics of the weight matrix remains the same as that of the initial random matrix.

Second, at each time step, a subset of neurons (15–20%) is active in the secondary layer. The rule strengthens the connections between the secondary-layer subset which *was* active at time $t - 1$ and the primary neurons that are active at time t . This reinforcement of feedback weights takes place at every time step while the primary layer is periodically stimulated. The effective feedback signal is given by the local field $\mathbf{h}^{(12)}$. During the first steps of the learning process the amplitude of this signal is weak, which means that the feedback influence is almost negligible. Then, as time goes on, the amplitude of the feedback signal grows, and then some values of $\mathbf{h}^{(12)}$ reach the critical threshold value $\theta^{(1)}$, and thus significantly increase the activation of the corresponding primary neurons. In order to estimate and represent the efficacy of this feedback signal, we consider the signal $\mathbf{F}^{(12)} = f_g(\mathbf{h}^{(12)} - \theta^{(1)})$, which corresponds to what would be the primary-layer activation if no input was sent. This signal is displayed in Fig. 3b, and compared with the current input signal $\mathbf{I}^{(1)}$.

One can remark that the input signal and the feedback signal are synchronized. Knowing that the transmission delay from secondary towards primary layer is equal to 1, the feedback signal at time t relies on the secondary pattern of activation at time $t - 1$, so that the secondary layer *anticipates* the activity of the primary

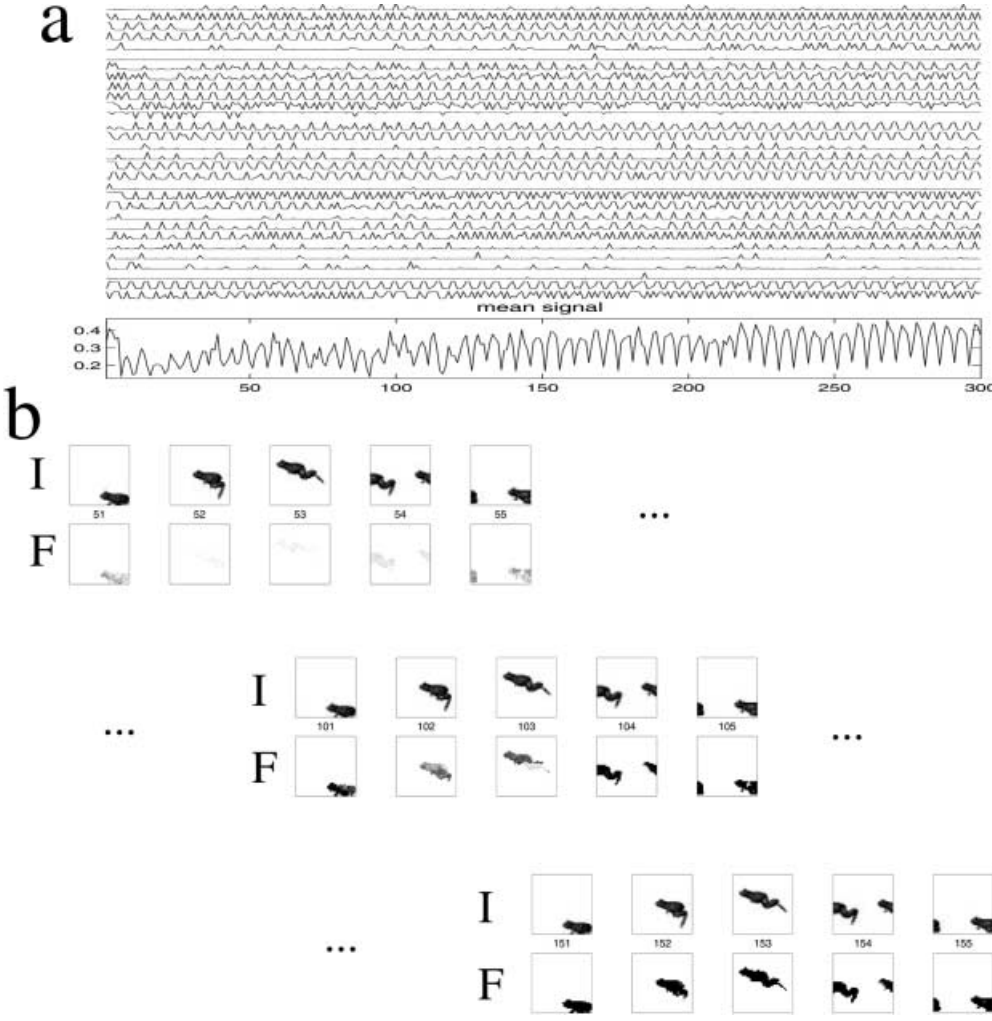


Fig. 3a,b. Learning dynamics, between $t = 1$ and $t = 200$ (with $N^{(1)} = 1600$ and $N^{(2)} = 200$). The system is continuously stimulated by a periodic spatiotemporal pattern (a frog jump). Parameters are in Table 1. **a** Neuronal activity in the secondary layer. Thirty individual signals (out of 200) are presented, and their mean activity is represented at the bottom. **b** Time evolution of input signal $I^{(1)}(t)$ and feedback signal $F^{(12)}(t)$ (see text), between $t = 51$ and $t = 155$ (for readability, most of the time steps have been discarded). At each time step, the 1600 values are represented as 40×40 images, where *white* corresponds to 0 and *black* to 1 (in-between values are gray)

layer. The feedback signal is thus a prediction on the forthcoming input, and corresponds to a “top-down expectation.”

The signal $F^{(12)}$ also provides an objective criterion for stopping the learning process. When the value of the feedback signal is as strong as the input signal, the learning process can be stopped so that one can test the recognition properties of the system (see Sect. 4.2). Note that the unbounded continuation of the learning process increases too strongly the amplitude of the feedback signal and the reduction of the inner dynamics, so that the system becomes insensitive to its input signal (and thus loses its adaptivity).

4.2 Recognition, retrieval, and dynamic memory

The aim of this section is to illustrate the computational abilities of our system. The reproducibility of these simulations has been checked on several networks.

For the sake of simplicity, we have performed learning on *elementary input sequences*. *Elementary* means that only one neuron is stimulated on the primary layer at a given time. The input sparsity is thus equal to $m_1^{(1)} = 1/N^{(1)}$. This choice helps to simplify notation and concentrates our attention on the temporal behavior of our system. A temporal input sequence is described by a

vector containing indices of neurons, $s = (i_1, \dots, i_\tau)$, so that $s(1) = i_1, \dots, s(\tau) = i_\tau$. The length of the sequence is τ . This sequence describes a periodic input signal of period τ , which is repeatedly presented between $t = t_1$ and $t = t_2$ ($t_2 \gg t_1$): $\forall t \in t_1, \dots, t_2, \forall j \in 1, \dots, N^{(1)}, I_j^{(1)}(t) = 1$ if $s[(t \bmod \tau) + 1] = j$, and $I_j^{(1)}(t) = 0$ otherwise.

4.2.1 Recognition. In this first example, we have learned one period-3 elementary sequence $[s = (1, 2, 3)]$. We then run the spontaneous dynamics (Eq. 1), and present different input signals, some of them corresponding to the learned sequence and others being unknown (Fig. 4). The point is to check that the feedback signal (i) is stimulus dependent and (ii) can adapt dynamically to its inputs.

During the 30 first steps, the input stimulus corresponds to the learned one. After 10–12 transient steps the system reaches its attractor, and the feedback signal is activated. At time $t = 32$ a phase shift occurs on the input signal. The mismatch between input and feedback signals leads to a transitory decrease of the feedback signal, which allows the inner dynamics to adapt to the input. After this new transient time, the feedback signal is again in synchrony with the input signal. Finally, at time $t = 62$, we reverse the time order of the input signal. In that case, the feedback signal fades out.

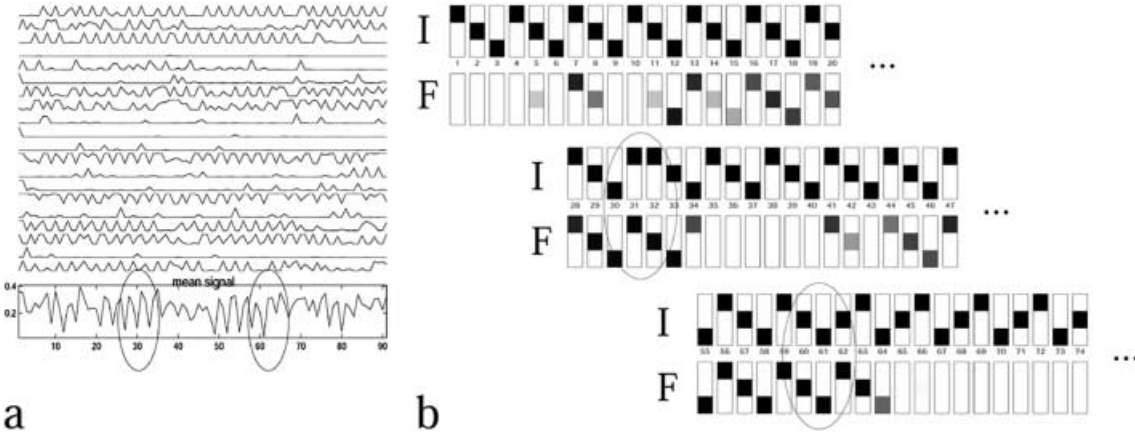


Fig. 4a,b. Activation dynamics, after learning the elementary sequence $s = (1, 2, 3)$, while presenting different stimuli. Input changes take place at $t = 31$ (input shift) and $t = 61$ (reverse temporal order). $N^{(1)} = 200$ and $N^{(2)} = 200$; other parameters are in Table 1. **a** Neuronal activity in the secondary layer. Twenty individual signals

are presented, with their mean activity. **b** Input signal (I) and feedback signal (F). Only the values corresponding to the first three primary neurons are presented, between $t = 1$ and $t = 74$ (some time steps have been discarded for readability)

So, one can remark that the activation of the feedback signal is very sensitive to the spatiotemporal structure of the input signal, i.e., it is *stimulus specific*: (i) it is grounded on a *coincidence detection* principle, i.e., to the detection of a specific spatial pattern of activations in the secondary layer; and (ii) the secondary-layer pattern of activation is stimulus specific, and is in particular highly sensitive to the time order of the input signal. For that reason, a change in the time order of the spatial inputs modifies the inner organization and thus deactivates the feedback signal. The system has thus learned to discriminate between one relevant stimulus and other non-relevant (nonlearned) stimuli (spatial and/or temporal mismatch – we have verified that a spatial mismatch deactivates the feedback signal in the same fashion).

When can we say that a system “recognizes” the input pattern? Most models that rely on resonant principles have to use a global attentional threshold which determines whether or not a new input pattern is coherent with previously learned patterns (Carpenter and Grossberg 1987). In our system, we define the *recognition* as the dynamic process which corresponds to the activation of a specific feedback signal. Recognition thus takes place without global control; it relies on the emergence of a specific dynamical configuration. It is thus more simple (or more “natural”) in its principle: the gating function is grounded on the coherent behavior of the whole population of neurons. The “decision” to recognize (or to ignore) a given stimulus comes from the collective activity of all the neurons belonging to the perceptual system.

4.2.2 Retrieval. One can now consider the conditions under which recognition takes place. The computational interest of a recognition process relies on the ability to determine the frontier between acceptance or rejection of the incoming signal, and then to explicit (or interpret) the accepted signals, i.e., to determine “what” is recognized. In Fig. 5 we use the same network as in the previous example. We then present two different input signals. Both of them are composed with the same

elementary single input, corresponding to the stimulation of the first primary neuron, but the time delay between those individual stimulations are different: the delay is 3 in the first case, like in the learned sequence, and 4 in the second case, which implies a temporal mismatch with the learned sequence. After a transient time, the system manages to fill the signal with the period-3 input. At time $t = 65$, a change in the input periodicity takes place, which leads to a progressive decrease of the feedback signal.

So, after learning, presenting a stimulus that has both spatial common points and a time coherency with the learned one leads the system towards a similar dynamical response, i.e., towards a similar attractor and a similar feedback signal (this similarity can be measured in terms of spatiotemporal correlation between samples of the compared patterns of activation). The system can thus *retrieve the missing information* according to a partial signal. (This retrieval ability also holds with spatially distributed inputs corrupted with a significant noise; Daucé (2000). The robustness to natural noise is tested in Sect. 5, in the case of a robotic application.) Otherwise, the sensitivity to the period-3/period-4 change illustrates the major influence of the inner signal on the response of the system. As the inner dynamics is strongly period sensitive, every change in the input period modifies the inner dynamical organization, and thus modifies the nature of the response.

4.2.3 Dynamical memory. One major feature of our system is its capacity to learn numerous different spatiotemporal patterns (see Sect. 4.3). Learning to recognize several spatiotemporal stimuli can lead to ambiguous situations, in particular when distinct input sequences have common features. In that case, some input signals are *spatially ambiguous*, i.e., they can be interpreted as belonging to two different sequences.

Figure 6 presents a system which has learned two distinct sequences: $s_1 = (1, 2, 3)$ and $s_2 = (3, 4, 5)$. These two sequences are 3-periodic and have in common the

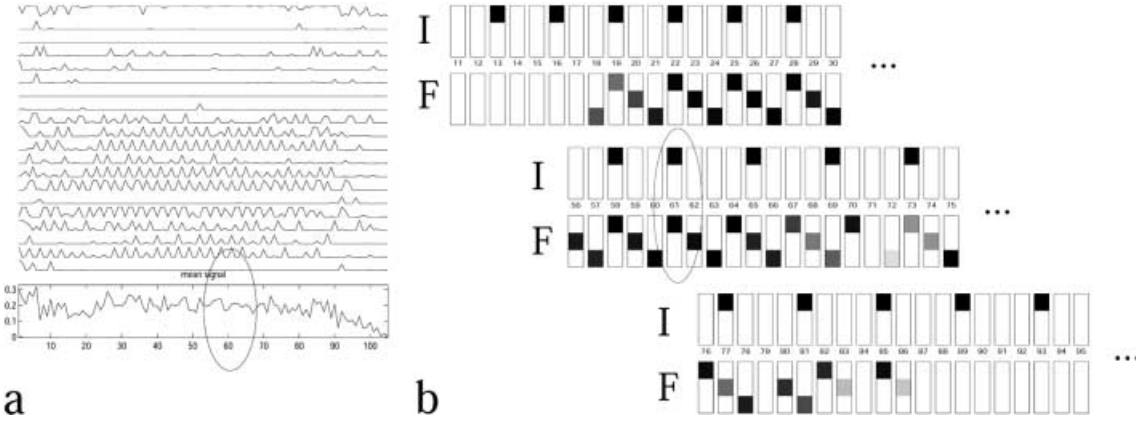


Fig. 5a,b. Feedback retrieval of the input pattern, after learning the elementary sequence $s = (1, 2, 3)$. Input change is perceptible at $t = 64$ (change in input periodicity). $N^{(1)} = 200$ and $N^{(2)} = 200$; other parameters are in Table 1. **a** Neuronal activity in the secondary layer. Twenty individual signals are presented, with their mean activity.

b Input signal (I) and feedback signal (F). Only the values corresponding to the first three primary neurons are presented, between $t = 11$ and $t = 95$ (some time steps have been discarded for readability)

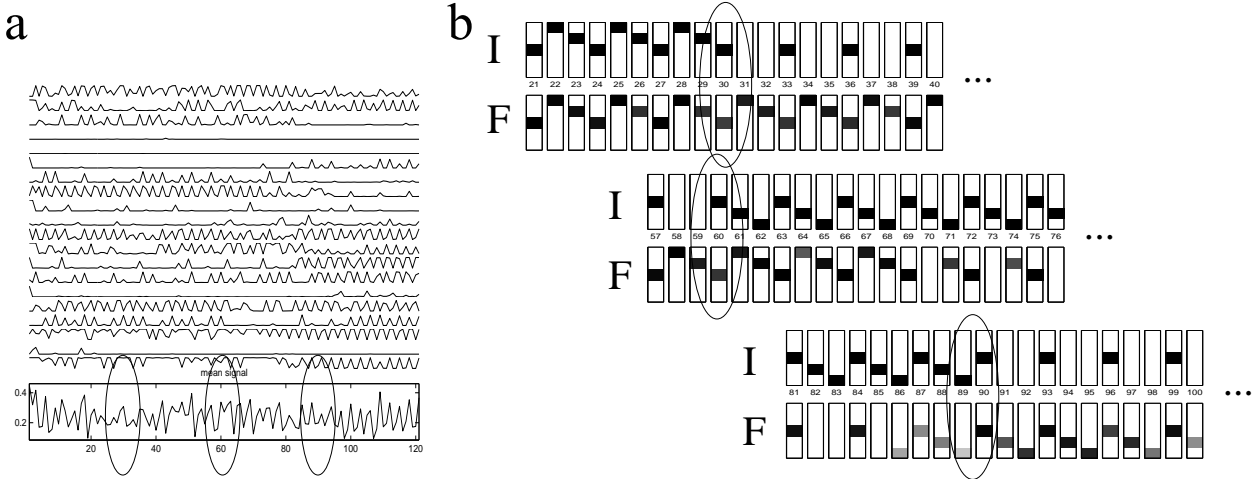


Fig. 6a,b. Dynamic memory (feedback retrieval depends on the past dynamics). Two sequences $s_1 = (1, 2, 3)$, $s_2 = (3, 4, 5)$, whose common element is “3,” have been learned. s_1 is presented between $t = 1$ and $t = 30$, $s_{\text{test}} = (0, 0, 3)$ is presented between $t = 31$ and $t = 60$, s_2 is presented between $t = 61$ and $t = 90$, and s_{test} is presented between $t = 91$ and $t = 120$. $N^{(1)} = 200$ and $N^{(2)} = 200$; other parameters are

in Table 1. **a** Neuronal activity in the secondary layer. Twenty individual signals are represented, with their mean activity. **b** Input (I) and feedback (F) signals. Only the values corresponding to the first five primary neurons are presented, between $t = 21$ and $t = 100$ (some time steps have been discarded for readability)

element “3.” The figure shows that the way the *same* dynamical sequence, $s_{\text{test}} = (3, 0, 0)$, is interpreted depends on previous stimulations: when the system is stimulated by sequence s_1 , it reaches an attractor associated to s_1 and interprets s_{test} as s_1 . When s_2 is presented, the system *changes its basin of attraction* and reaches the one associated to s_2 , so that s_{test} is now interpreted as s_2 . In that particular example, one can remark that the time necessary to reach the second attractor is rather long, i.e., the presentation of the second stimulus during 30 time steps (from $t = 61$ to $t = 90$) is just long enough for stabilizing the response of the system on the second attractor.

Particularly interesting is the global *remapping* that one can observe in the secondary layer (Fig. 6a). The change in the inner organization is perceptible around $t = 80$ (20 steps after the presentation of s_2), and one can see that the activities of the secondary neurons change

qualitatively (some neurons become silent, other become more active). This different inner organization explains that one can have a different feedback response when the same stimulus s_{test} is presented. So, this example shows that the way a given signal s_{test} is interpreted does not only depend on its own intrinsic values, but also on a context that can be memorized in an attractor. In that sense, our system has a *memory* of past events.

We have shown that after learning one or several stimuli, our system exhibits new computational abilities: the ability to discriminate between familiar and unknown stimuli, the ability to recognize and retrieve partial signals, and the ability to store in the dynamics the memory of past events. Those properties are grounded on the temporal behavior of the system, and for that reason they are highly sensitive to the time relationships and to the periodicity of the presented stimuli. Because they rely on a dynamical system, they

also need several time steps for the system to converge towards its attractor, and the response at a given time is not only guided by the input, but also by inner dynamical constraints.

One can say that the computational abilities of our systems are astonishingly complex, knowing that we start from a rather simple design. One can now ask the question of capacity; i.e., how many stimuli can be stored and retrieved in a single system?

4.3 Capacity

The number of different spatial input patterns that can be memorized in recurrent attractor systems, such as Hopfield systems, is generally found to be linearly dependent in N . One thus defines a capacity criterion $\alpha_c = n_c/N$, where n_c is the maximal “critical” number of spatial patterns that can be learned. For a given value of N , when one tries to learn more than $\alpha_c N$ spatial patterns, the retrieval ability suddenly decreases (“catastrophic” forgetting).

Starting from a tabula rasa, one can also store spatiotemporal periodic patterns instead of spatial patterns in recurrent systems (Herz et al. 1989). Basically, individual neurons work as coincidence detectors, and tend to react specifically to the coactivation of a given set of presynaptic neurons. Globally, one can observe chains of firing, leading to a stable spatiotemporal activation pattern (Hermann et al. 1995). When such chains are closed, every different loop corresponds to a different periodic (cyclic) attractor. The capacity of such systems is subject to the same constraints as Hopfield systems, and is also defined as the number of spatial patterns that can be stored, independently of their temporal succession. Theoretical estimates of the capacity of such systems can be found in Meunier and Nadal (1995) and Hermann et al. (1995).

In our systems, there is no explicit storage of spatiotemporal sequences. The retrieval relies on two mechanisms: (i) the decrease of chaos (i.e., increase of predictability) between the activities of the primary and secondary layers (which is necessary for the robustness of the response), and (ii) a coincidence-detection mechanism from the secondary layer towards the primary layer (which activates or disables the feedback signal). In order to allow comparison with existing models, we define a measure of capacity that relies on this retrieval mechanism. The “knowledge” of a given sequence of inputs thus manifests in the network ability to activate a feedback signal which is coherent with the input signal. For an estimation of the capacity, we only refer to the size of the secondary layer $N^{(2)}$, since the size of primary layer has no influence on the retrieval properties of the system.

During the training process, a spatiotemporal sequence s_1 is repeatedly presented until our learning mechanism (Eq. 2) produces an active feedback signal. Then we test the correlation between input and feedback signals for that particular sequence (with dynamics as in Eq. 1); i.e., $\forall t > 0, r_{1,1}(t) = \text{cor}[\mathbf{I}^{(1)}(t), \mathbf{F}^{(12)}(t)]$ and

$r_{1,1} = (1/T) \sum_{t=1}^T r_{1,1}(t)$, with $T \gg 1$. If $r_{1,1}$ is close to 1, input and feedback signals are found to overlap. Then a second sequence is learned, then a third one, ..., then a k th one. The period of the k th sequence is chosen between 3 and 7, i.e., $\tau_k \in \{3, 4, 5, 7\}$, with equal probability. At step k , we measure the retrieval for every previously learned sequence, i.e., for $m = 1, \dots, k$, we calculate $r_{m,k}$. For every value of $k > 0$, the total number of spatial patterns that constitute the learned sequences is equal to $n_k = \sum_{m=1}^k \tau_m$. The mean retrieval among all learned sequences is equal to $r_k = (1/k) \sum_{m=1}^k r_{m,k}$. When r_k is close to one, the retrieval is good for almost every sequence. When r_k is close to zero, the ability to retrieve any of the learned sequences is null, which corresponds to a “catastrophic forgetting.”

This experiment has been carried out on ten networks (Fig. 7a) with elementary sequences (and without overlap between the spatial patterns composing the sequences). The size of the secondary layer is $N^{(2)} = 200$, and learning only takes place on feedback links (i.e., $\varepsilon^{(22)} = 0$). For every network, r_k is plotted in function of n_k . Globally, the shape of the curves is similar for every network, with good retrieval for low values of n_k , and a sudden decrease towards zero. So, one can estimate, for a given network, a critical value n_c (corresponding to the sudden decrease) such that $\alpha_c = n_c/N^{(2)}$. There are significative differences between individual networks (i.e., n_c is between 120 and 180), and the mean capacity α_c is found to be approximately 0.7.

The shape of the curves and the value of α_c strongly vary depending on the parameters settings. We have tried on the following experiments to estimate the role of $\varepsilon^{(22)}$ (the inner-links learning parameter; Fig. 7b), $N^{(2)}$ (the size of the secondary layer; Fig. 7c), and $m_{1z}^{(1)}$ (the sparsity of the spatial input patterns; Fig. 7d).

Parameter $\varepsilon^{(22)}$ relates to the process of dynamics reduction. The larger $\varepsilon^{(22)}$ is, the less chaotic (more predictable) is the response of the system after learning. The link between this increase of predictability and the increase of robustness to noise has been shown in simpler learning situations (Dauvé et al. 1998). It has also been shown that this increase of robustness is costly; i.e., an increase of robustness induces a decrease of capacity. The same dilemma holds on the present model. We can see in Fig. 7b that an increase of parameter $\varepsilon^{(22)}$ has a counterpart in terms of capacity: the more stable is the response, the lower is the capacity. One has to find a compromise between stability and capacity. For the experiments carried out in Sect. 4.2, we have taken $\varepsilon^{(22)} = 0.02$, which corresponds to a capacity of approximately 0.5.

The size effects are displayed in Fig. 7c, again with elementary sequences and $\varepsilon^{(22)} = 0.02$, for different values of $N^{(2)}$. With small fluctuations from one network to the other, we find again a capacity of approximately 0.5.

Finally, we measured the effect of cross-overlap between spatial patterns composing the sequences. The spatial input patterns are assumed sparse (i.e., a small proportion of primary neurons are stimulated at the same time), so that cross-overlap between spatial input

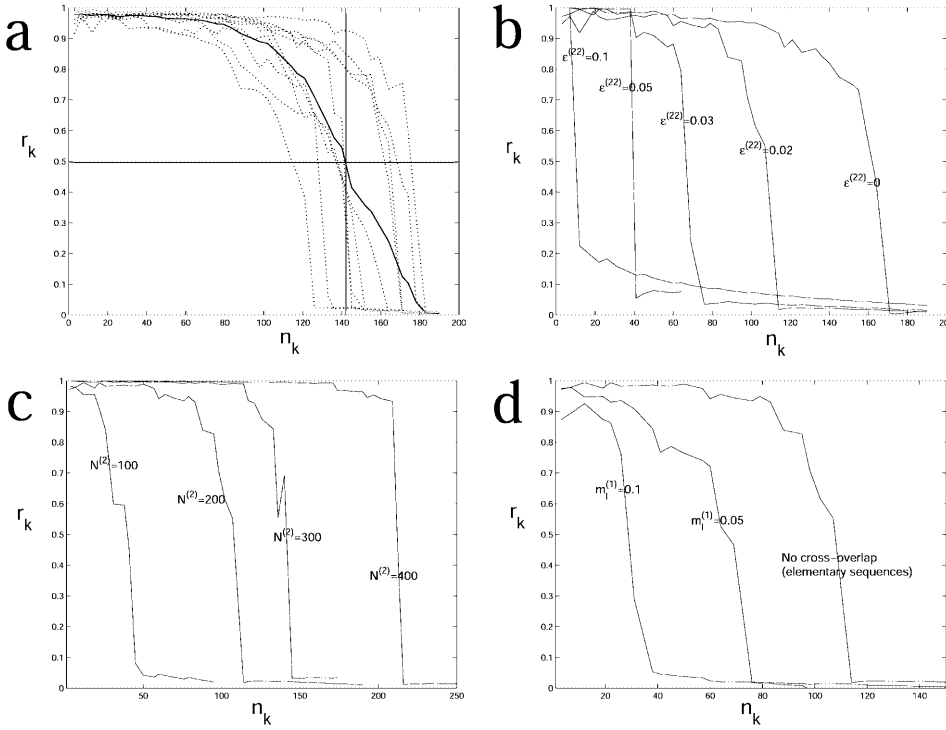


Fig. 7a–d. Different measures of the capacity of the model. r_k is plotted as a function of n_k (see text). Nonspecified parameters are in Table 1. **a** Interindividual variability, for elementary sequences learning, with $\epsilon^{(12)} = 0.1$, $\epsilon^{(22)} = 0$, and $N^{(2)} = 200$. *Dotted lines* correspond to individual networks, *solid line* corresponds to the mean over the ten networks. **b** Measures of capacity for different values of $\epsilon^{(22)}$, for elementary sequences learning, with $\epsilon^{(12)} = 0.1$ and $N^{(2)} = 200$. **c** Measures of capacity for different values of $N^{(2)}$, for elementary sequences learning, with $\epsilon^{(12)} = 0.1$ and $\epsilon^{(22)} = 0.02$. **d** Measures of capacity for different values of input sparsity $m_1^{(1)}$, with $\epsilon^{(12)} = 0.1$, $\epsilon^{(22)} = 0.02$, and $N^{(2)} = 200$.

patterns is weak. When we use elementary sequences, this cross-overlap is null. In Fig. 7d, we measure the capacity when spatial input patterns are chosen according to a random draw, so that $\mathcal{P}(I_i^{(1)}(t) = 1) = m_1^{(1)}$ and $\mathcal{P}(I_i^{(1)}(t) = 0) = 1 - m_1^{(1)}$. In that case, the cross-overlap between spatial patterns is of the order of $(m_1^{(1)})^2$. Figure 7d shows that cross-overlap induces a sensible decrease of capacity. For instance, when $m_1^{(1)} = 0.05$ (which approximately corresponds to the “frog” sequence of Fig. 2), the capacity is approximately 0.3 (i.e., when $N^{(2)} = 200$, the system should be able to learn and discriminate approximately eight spatiotemporal sequences analogous (statistically) to the frog sequence).

These experiments have shown that our system can display high capacity (of approximately 0.7) in the best case, but real-world systems both need reliability of response, and robustness to noise and cross-overlap. Under these more realistic constraints, the capacity of our system is found to be approximately 0.3. In Sect. 5 we consider the real-world implementation of sensory–motor associations on a robotic task.

5 Robot experiment

We present here a prototypic experiment (performed on a *real* robot) that illustrates the ability of the ReST architecture to link spatial and temporal relationships, which provides a basis for robot navigation architectures. Our aim is not to solve a new hard robotics problem, but to clarify the way our system could lead to real-world applications.

We take into account the following classical requirements for the building of adaptive navigation systems:

1. The system needs to maintain *stable behaviors* in a changing environment. The use of attractor system may be suitable for this requirement (Schöner et al. 1995).
2. The learning of new behaviors may be grounded on real data. Every new behavior should have a matching correspondence with a class of real sensory–motor situations (Varela et al. 1991; Kuniyoshi and Bertouze 1998; Tani and Nolfi 1998).

5.1 Three-layer sensory–motor model

The basis of the control architecture is the Perac block designed by the ETIS team (Gaussier and Zrehen 1995). The platform is a Koala robot supplied by K-Team (Preveranges, Switzerland). The idea here is to build primary layers which both display external signals to the secondary layer and receive a signal from it, thus interpreting inner dynamic responses. In this case we have two primary layers, one corresponding to visual perception and the other corresponding to the perception of motor movements. We thus have a system with $P = 3$ populations, with index 1 corresponding to the visual primary layer, index 2 corresponding to the secondary layer, and index 3 corresponding to the motor primary layer (see Fig. 8). In our experiment the parameters are as follows: $N^{(1)} = 90$, $\theta^{(1)} = 0.5$, $N^{(2)} = 100$, $\theta^{(2)} = 0.4$, $N^{(3)} = 7$, $\theta^{(3)} = 0.5$, and $g = 8$.

Visual input. A CCD camera captures pictures of the environment. High curvature points (eg., corners) are extracted from the gradient of the image. In a navigation context, the correspondence between a salient point (called now a “landmark”) with its angular position (azimuth) in respect with an absolute direction (north as

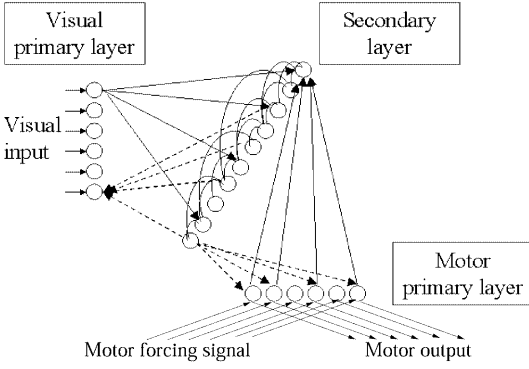


Fig. 8. ReST architecture for perception-action systems. The initial primary layer has been split into two perceptual layers: visual primary layer and sensory-motor primary layer. The fusion of visual and motor information is processed by the secondary layer

given by a compass) gives the position of that landmark in the environment. At each time step, a set of five azimuths, corresponding to the five more-salient landmarks in the input image, constitutes the visual input $I^{(1)}$ (the angular confidence interval is 4° , so that the number of visual entries is $N^{(1)} = 90$).

Motor input. In this experiment, the robot movements are limited to seven possible rotations from -90° to 90° , in 30° steps. The motor layer is composed of $N^{(3)} = 7$ neurons, each associated with one motor command, so that the neuron with maximal activation determines the movement. The robot is thus limited to rotations, in order to allow simple correspondences between the motor movements and the visual field.

Learning is achieved with a forcing motor signal on layer 3. The purpose is to link (associate) this motor flow with the incoming visual flow. As in previous simulations, we use a periodic signal. This motor signal corresponds to the 3-periodic sequence of rotations $(+30^\circ, +60^\circ, +90^\circ)$, so that after three steps, the robot has made a half turn; and after six steps, the robot faces its initial visual field. Apart from visual noise and small angular shifts, the visual input signal is thus supposed to be of period 6 (Fig. 9).

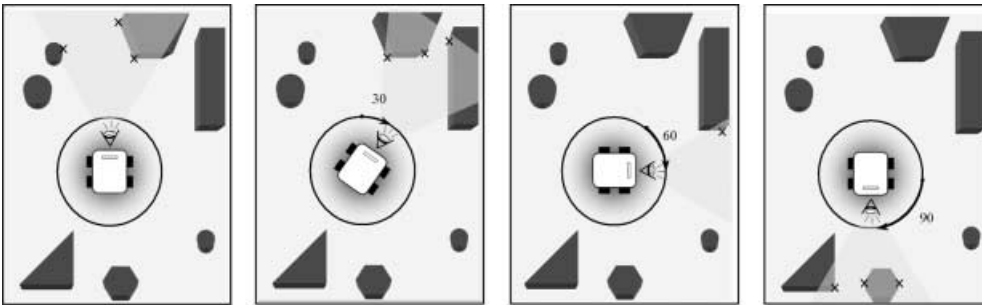


Fig. 9. Successive positions of the robot after a motor command sequence $(+30^\circ, +60^\circ, +90^\circ)$. The robot stands in an open environment (this is not a simulation). The association of a set of landmarks (high curvature points, denoted by x) with their angular positions

5.2 Learning and recognition

There are two stages in the training process. During the first 20 steps, we iterate the dynamics (Eq. 1) with the forcing motor signal, without changing the weights, until the system reaches its stationary dynamics. After this transient time, we activate the learning rule (Eq. 2). Due to friction between the wheels and ground, the actual rotation is slightly different from the command issued. Therefore, during the whole training process we check the accuracy of the angular position (we correct the position when the difference is too large). The learning dynamics lasts 20 time steps (one time step corresponds to one movement). This training session is not long enough to produce a sustained feedback signal, as in previous simulations. However, the feedback signal from layer 2 to layer 3 is stable enough to determine the motor output of the system when the forcing signal is removed.

After this learning process, the resulting system is tested with the dynamics as in Eq. (1). The forcing motor signal is removed, so that the robot now determines its movement according to the feedback signal $F^{(32)}(t)$. The robot is initially placed in an arbitrary angular direction. Two typical angular “trajectories” are reported in Fig. 10. After some transients, the robot starts to reproduce the 3-periodic sequence of rotations. This periodic movement occurs as soon as the robot finds a matching correspondence with its visual entries, and remains as long as visual inputs and motor commands match each other. In the first experiment (Fig. 10a), the reaching of the periodic behavior is followed by a progressive shift in the robot orientation. As a consequence, visual information progressively tends to be mismatched with the learned sequence of visual patterns (as the visual angle is of the order of 60° , a position mismatch of approximately 30° corresponds to an “error” of 50% in the visual field). This increasing *conflict* between movement and vision leads to a *sudden change* in the robot behavior. One movement does not take over the other, but for some time steps the movements performed do not follow the sequence anymore, nor correspond to the ones associated with the image. After these new transients, the robot finally finds a matching visual input, triggers the associated movement, and resumes again the

constitutes the visual input. After three commands the robot is facing backwards (issuing these commands again let the robot face its initial visual scene)

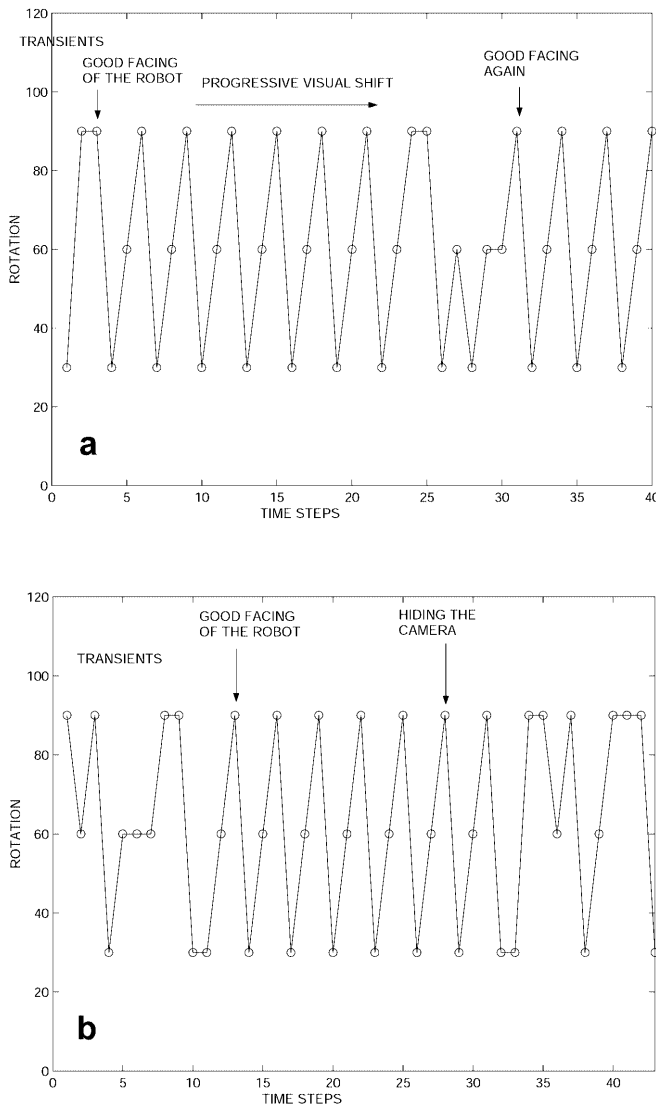


Fig. 10a,b. Angular trajectories of the robot; rotation angle versus time. **a** Example of recalibration after a shift. The first two steps are transients, then the rotations issued correspond to the learned periodic sequence ($+30^\circ$, $+60^\circ$, $+90^\circ$) in accordance with its associated visual inputs (so that vision and movements are dynamically locked). Due to friction on the ground, the real robot angle (and thus the visual scene) shifts, leading to a progressive mismatch between the visual scene and the movement. One can observe a sudden change in the robot behavior (at $t = 25$), corresponding to an unlock between the visual flow and the associated movements. Finally, after new transients, the robot finds a good match and resumes the periodic sequence. **b** After the robot has reached its periodic behavior, and the camera is hidden. The lack of visual information rapidly leads the robot to a “chaotic” behavior

correct sequence. The movement performed by the robot in this conflict state are still of 30° , 60° , and 90° rotations. There is no error calculation between the desired rotation and the effective rotation which could lead to other rotation angles. However, erratic rotation and friction allow visual fields that are close enough to a learned one to be reached, so that the learned sequence of movements can start again. In the second experiment (Fig. 10b), we simply hide the camera after the robot has

reached its periodic behavior. The lack of visual information thus produces erratic rotations, and the robot keeps searching for a matching visual input.

As we can see, our system can produce two distinct behaviors that both depend on its visual environment and its actual movement. By analogy, one can interpret movements performed in the context of dynamical systems; the change in behavior is comparable to a *phase transition* from a cyclic dynamics towards a chaotic dynamics:

1. The learned periodic movement corresponds to a *task* associating visual inputs and motor movements. It is *stable* for a broad range of visual inputs, including shifted visual inputs.
2. The “chaotic” movement can be seen as an *exploratory behavior* – the search for matching visual input sequences. When there is no possible match (for instance when the scene is hidden, or when the robot is moved to another place), the dynamics remains chaotic.

This preliminary experiment shows that our system can perform reliable sensory–motor associations in a real environment (e.g., including noise on the visual input, and visual shifting due to the ground friction). These associations are based on an on-line learning process, without a priori knowledge of the environment configuration. The secondary dynamical layer allows the fusion of visual and motor information, and is responsible for the stability of the control schemes, and for the dynamical adaptivity in cases of strong mismatch (the experiment is analogous to the simulation presented in Fig. 4). It globally models the coupling between the agent and the environment in a repetitive sensory–motor task.

In order to go further in the design of navigation systems, several strategies should be explored:

1. In more-complex task processing, one needs to learn sensory–motor associations and environment couplings at broader temporal scales: (i) the memory of previous behaviors may, for instance, constrain the choice of the actual behavior, as in Fig. 6; and (ii) the question of learning longer sensory–motor schemes is still open, and would need a broader range of axonal delays for individual neurons (see also Herz et al. (1989) for a discussion on delays).

2. Our model requires the repetition of a sensory–motor scheme in order to learn it – it is not assumed to perform “one-shot learning” (i.e., the ability to store a particular event in emergency conditions). However, using the autonomous dynamics, we could allow the system to rest in order to store and replay (with an inner dynamic feeding) some specific critical or emotional sensory–motor configuration (“mental rehearsal,” see also Tani and Nolfi 1998).

3. The learning of *nonperiodic* behaviors may rely on the emergence of sensory–motor schemes in a nonsupervised learning task. Reinforcement learning methods (which relate to the pleasure or the pain associated with some particular events) are currently under experimen-

tation using our model, where the learning parameters $\varepsilon^{(pq)}$ are functions of some external reinforcement.

6 Discussion

We have presented a model where dynamical encoding and processing cannot be reduced to a simple feedforward process. Our system is recurrent, and consequently presents an operational closure (Varela et al. 1991), so that the inner constraints dominate the external signal. One can also say that the inner dynamics corresponds to a “simulation” of the external world, which is updated according to the input signal. In any case, the traditional input–output dependency is modified: *the predictability of a sensory–motor scheme is dependent on the fitting between the inner dynamics and the input–output flow*. When such fitting is observed (dynamic or structural coupling, or resonance), one can predict the behavior of the whole system as in traditional input–output systems. On the contrary, when the fitting is poor, the whole system is found to produce complex inner dynamics and unpredictable sensory–motor behaviors.

Even if the link with biology is a delicate matter with our simple analog neuronal units, we will attempt to provide some plausible analogies with real biological neural structures and functions, and also to estimate the limits of such analogy.

The question of recognition is central in our system, and corresponds to “acceptance” or “rejection” of some spatiotemporal configurations arriving on the primary layers. Most of the signals are rejected, or ignored, while some of them allow the activation of a specific resonant feedback signal. This property relates to the question of dynamic binding (von der Malsburg and Schneider 1986; Bienenstock and Geman 1995), i.e., the ability to link together separate elements. In our model, the individual elements constituting a sequence are not significant by themselves. The activation of a feedback signal needs a specific spatiotemporal disposition of these individual elements, which are thus processed and “perceived” as a whole. This hypothesis of dynamic binding is present at different scales in neurophysiological studies (Gray and Singer 1987; MacLeod and Laurent 1996; Rodriguez et al. 1999). Our model is one of the possible implementations of the dynamic binding hypothesis, and thus is a candidate for explaining how such binding occurs in the brain.

The possible role of chaotic dynamics in brain processing is also a matter of interest for neurophysiologists. The principal hypothesis on the functional role of chaos in olfactory perception systems was stated by Skarda and Freeman (1987). In their article, they interpret the recognition of an olfactory stimulus as the stabilization of an unstable orbit of a chaotic attractor. Chaos is thus seen as a reservoir of cycles, where every unstable orbit corresponds to the encoding of a specific odor. Our model is not fully compatible with Skarda and Freeman’s model, even if the ideas are globally comparable. In particular, since the input dynamics takes part in the dynamic process, the different attractors associ-

ated with different stimuli do not correspond to a subpart of a global chaotic attractor. In our model, due to structural instability there is no global attractor, but instead many transitions between distinct attractors, chaotic or not, depending on the input signal, the inner constraints, and previous learning.

It is difficult to claim strong links between our model and some specific cortical or subcortical regions. However, the 3-populations ReST model, which is devoted to navigation, has connections with the hippocampus architecture. Other work by the ETIS team has already taken inspiration from the hippocampal architecture for the design of control architecture for the Koala mobile robot (Revel et al. 1999; Gaussier et al. 2000). The ReST model has been inserted in this architecture and takes the place of the area denoted as CA3. Structurally, this area is known for its important recurrent links. Functionally, it has been found to display a functional remapping in case of environmental contextual changes (Barnes et al. 1997), and it is supposed to be the place where locations and/or temporal sequences are learned when the animal is performing an action. These observations and hypotheses are compatible with the dynamical organization and computational abilities of our system. This analogy has to be investigated more deeply, but may already give new insights in the way the CA3 region processes information.

In the same way, the analogy with the visual system (V1 and V2) is not straightforward, but our model may provide clues to those interested in the role of feedback links in visual perception. First, it is known that 80% of the entries in the lateral geniculate nucleus correspond to feedback connections from the visual cortex. According to Crick (1984), this feedback information enhances the sensitivity of some neurons, according to the expectations of the cortex on the visual flow. Second, some recent studies (Hupé et al. 1998) have shown that V2 to V1 feedback connections may play a role in the processing of figure–ground segregation. Some theoretical models have been proposed (e.g., Ross et al. 2000) for explaining the psychological phenomenon of illusory contour detection. Our model, even coarser, brings the idea that feedback signal may also be implied in the reinforcement – by anticipation – of the primary treatment of dynamic scenes and objects.

Finally, one can consider the temporal scales of the phenomena we want to model. This question is not trivial. Our system uses its own discrete-time parallel updating, which is not associated with a particular temporal unit. The timescale is not defined a priori, so that one has to consider the specific field of application to determine an “external” temporal reference. The visual and perceptual analogies suggest interpreting the synchronization and dynamic binding on a millisecond timescale. On the contrary, sensory–motor experiments take place in the range of seconds. In future work with the same global structures it may be necessary to distinguish between the modeling of sensory perception, using spiking neurons with biologically compatible timescales, and control models that may correspond to the modeling of global structures, on larger timescales.

Nevertheless, the compatibility between these two interpretations illustrates the genericity and “universality” of our model of dynamical perception.

Acknowledgements. This work was supported by a French GIS contract on cognitive sciences entitled “Dynamical coding of information by asymmetric recurrent neural networks.” The collaboration includes the following laboratories: ETIS, Cergy-Pontoise (M. Q.-P. Gaussier); ONERA-CERT, Toulouse (E. D.-M. Samuelides); INSERM U455, Toulouse (B.D.); and INLN, Nice (B. Cessac). We would like to thank all these colleagues for helpful comments and discussions.

References

- Ables M, Bergman H, Margalit E, Vaadia E (1993) Spatiotemporal firing patterns in the frontal cortex of behaving monkeys. *J Neurophysiol* 70: 1629–1638
- Amari S (1972) Characteristics of random nets of analog neuron-like elements. *IEEE Trans Syst Man Cybern* 2: 643–657
- Barnes CA, Suster MS, Shen J, McNaughton BL (1997) Multistability of cognitive maps in the hippocampus of old rats. *Nature* 388: 272–275
- Bienenstock E, Geman S (1995) Compositionality in neural networks. In: Arbib M (ed) *The handbook of brain theory and neural networks*. MIT Press, Cambridge, Mass., pp 223–226
- Carpenter GA, Grossberg S (1987) A massively parallel architecture for a self-organizing neural pattern recognition machine. *Comput vis graph image process* 37: 54–115
- Cessac B (1995) Increase in complexity in random neural networks. *J Phys I* 5: 409–432
- Crick F (1984) Function of the thalamic reticular complex: the searchlight hypothesis. *Proc Natl Acad Sci USA* 81: 4586–4590
- Daucé E, unpublished observation, 2000
- Daucé E, Quoy M, Cessac B, Doyon B, Samuelides M (1998) Self-organization and dynamics reduction in recurrent networks: stimulus presentation and learning. *Neural Netw* 11: 521–533
- Daucé E, Moynot O, Pinaud O, Samuelides M (2001) Mean-field theory and synchronization in random recurrent neural networks. *Neural Process Lett* 14: 115–126
- Doyon B, Cessac B, Quoy M, Samuelides M (1993) Control of the transition to chaos in neural networks with random connectivity. *Int J Bifurc Chaos* 3: 279–291
- Elman JL (1990) Finding structure in time. *Cogn Sci* 14: 179–211
- Gaussier P, Zrehen S (1995) Perac: A neural architecture to control artificial animals. *Robot Auton Syst* 16: 291–320
- Gaussier P, Joulain C, Banquet J, Leprêtre S, Revel A (2000) The visual homing problem: an example of robotics/biology cross fertilization. *Robot Auton Syst* 30: 155–180
- Gerstner W, Ritz R, van Hemmen J (1993) A biologically motivated and analytically soluble model of collective oscillations in the cortex. I. theory at weak locking. *Biol Cybern* 68: 363–374
- Gray C, Siger W (1989) Stimulus specific neural oscillations in orientation columns of cat visual cortex. *Proc Natl Acad Sci USA* 86: 1698–1702
- Hermann M, Hertz J, Prugel-Bennett A (1995) Analysis of synfire chains. *Network* 63: 403–414
- Hertz J, Prugel-Bennett A (1996) Learning synfire chains: turning noise into signal. *Int J Neural Syst* 7: 445–450
- Herz A, Sulzer B, Kuhn R, van Hemmen JL (1989) Hebbian learning reconsidered: representation of static and dynamic objects in associative neural nets. *Biol Cybern* 60: 457–467
- Hopfield JJ (1982) Neural networks and physical systems with emergent collective computational abilities. *Prob Nat Acad Sci USA* 79: 2554–2558
- Hupé J-M, James A, Payne B, Lomber S, Girard P, Bullier J (1998) Cortical feedback improves discrimination between figure and background by V1, V2, and V3 neurons. *Nature* 394: 784–787
- Kuniyoshi Y, Berthouze L (1998) Neural learning of embodied interaction dynamics. *Neural Netw* 11: 1259–1276
- MacLeod K, Laurent G (1996) Distinct mechanisms for synchronization and temporal patterning of odor-encoding neural assemblies. *Science* 274: 976–979
- Malsburg C von der, Schneider W (1986) A neural cocktail-party processor. *Biol Cybern* 54: 29–40
- Meunier C, Nadal J-P (1995) Sparsely coded neural networks. In: Arbib M (ed) *The handbook of brain theory and neural networks*. MIT Press, Cambridge, Mass., pp 899–901
- Moynot O, Samuelides M (2002) Large deviations and mean-field theory for asymmetric random recurrent neural networks. *Probab Theory Relat Fields* 123 1: 41–75
- Revel A, Gaussier P, Banquet J (1999) Taking inspiration from the hippocampus can help solving robotics problems. In: *Proceedings of the European Symposium on Artificial Neural Networks*, Bruges, Belgium, 21–23 April, pp 357–362
- Rodriguez E, George N, Lachaux J-P, Martinerie J, Renault B, Varela FJ (1999) Perception's shadow: long-distance synchronization of human brain activity. *Nature* 397: 430–433
- Ross WD, Grossberg S, Mingolla E (2000) Visual cortical mechanisms of perceptual grouping: interacting layers, networks, columns, and maps. *Neural Netw* 13: 571–588
- Schillen T, König P (1991) Stimulus dependent assembly formation of oscillatory responses: II. desynchronization. *Neural Comput* 3: 167–178
- Schöner G, Dose M, Engels C (1995) Dynamics of behavior: theory and applications for autonomous robot architectures. *Robot Auton Syst* 16: 213–245
- Sejnowski TJ (1977) Strong covariance with nonlinearly interacting neurons. *J Math Biol* 4: 303–321
- Skarda C, Freeman W (1987) How brains make chaos in order to make sense of the world. *Behav Brain Sci* 10: 161–195
- Sompolinsky H, Crisanti A, Sommers H (1988) Chaos in random neural networks. *Phys Rev Lett* 61: 259–262
- Tani J, Nolfi S (1998) Learning to perceive the world as articulated: an approach for hierarchical learning in sensory-motor systems. In: Pfeifer R, Blumberg B, Meyer J, Wilson S (eds) *From animals to animats: simulation of adaptive behavior*. MIT Press, Cambridge Mass., pp 270–279
- Thorpe SJ, Fize D, Marlot C (1996) Speed of processing in the human visual system. *Nature* 381: 520–522
- Varela F, Thompson E, Rosch E (1991) *The embodied mind*. MIT Press, Cambridge, Mass
- Williams RJ, Zipser D (1989) A learning algorithm for continually running recurrent neural networks. *Neural Comput* 1: 270–280